Stress distribution according to the design of slot cover

in aesthetic passive self-ligating bracket

: a finite element analysis

Moonhee Kim

The Graduate School

Yonsei University

Department of Dentistry

Stress distribution according to the design of slot cover in aesthetic passive self-ligating bracket : a finite element analysis

A Dissertation

Submitted to the Department of Dentistry

and the Graduate School of Yonsei University

in partial fulfillment of the requirements for the degree of

Doctor of Philosophy of Dental Science

Moonhee Kim

June 2024

This certifies that the Dissertation Thesis of

Moonhee Kim is approved.

Thesis Supervisor, Kee-Joon Lee

Jung-Yul Cha

Sung-Hwan Choi

Jee-Hwan Kim

Jae-Sung Kwon

The Graduate School

Yonsei University

June 2024

감사의 글

먼저, 돌아온 탕자와도 같은 저에게 소중한 기회를 주셔서 포기하지 않고 지금 이 글을 쓸 수 있도록 허락 해 주신 이기준 학장님께 깊은 감사와 존경의 마음을 드립니다.

많이 모자란 저를 세심하게 지도 해 주신 차정열 과장님, 원내생 시절부터 늘 따뜻하게 이끌어 주셨던 최성환, 김지환 교수님, 더불어 기본적인 부분부터 친절히 조언 해 주신 권재성 교수님 덕분에 20여년 전 어느 눈 내리던 겨울 날, 합격자 발표 순간의 전율로부터 지금 이 순간 까지 늘 저에게는 자랑이자 그리움이었던 아름다운 모교에서 늦었지만 미약하나마 방점을 찍을 수 있게 되어 감격스럽습니다.

치과교정과 의사의 길을 걷게 해 주신 영원한 멘토 전윤식 교수님, 사랑으로 지도 해 주신 박선형, 김민지 교수님, 직접 저를 치료 해 주셔서 처음 교정학의 길을 소개해 주신 유형석 교수님, 아무 것도 모르던 학부 시절부터 많은 가르침을 주셨던 박영철, 백형선, 황충주, 김경호, 최광철, 정주령, 최윤정, 김하림 교수님 이하 교실의 모든 큰 스승 님들께 항상 감사한 마음을 새기며 앞으로도 바른 마음으로 겸손하고 성실히 정진하겠습니다.

끝으로 철 없는 아들을 항상 지지해 주시는 부모님과 하나 뿐인 누나에게 마지막 졸업장을 바치며, 이 소중한 성취를 허락하신 모든 것 주관하시는 하나님께 영광 돌립니다.

2024년 6월

저자 씀

TABLE OF CONTENTS

LEGENDS OF FIGURES

LEGENDS OF TABLES

ABSTRACT

Stress distribution according to the design of slot cover in aesthetic passive self-ligating bracket : a finite element analysis

Moonhee Kim

The Graduate School of Yonsei University

Department of Dentistry

(Directed by Professor Kee-Joon Lee)

Since aesthetic passive self-ligating brackets fabricated entirely of ceramic are widely adopted, it is crucial to evaluate the stress distribution related to fracture due to the inherent properties of material itself. This study compares the stress distribution and their characteristics of three finite element models: two reverse-engineered models of existing representative brackets with different design of slot cover, keyhole type (bracket A) and drawer type (bracket B), and a newly designed dovetail type (bracket C), which is modified for better rotational control, fracture resistance, and cost efficiency with a simplified structure.

Tensile stress distribution on the areas of interest under specific compressive load was compared, and then visualized and numerically analyzed simulating several clinical situations divided into extreme and relatively general conditions with orthodontic archwires.

The body of the bracket C showed lower tensile stress, especially on the slider, whereas its clip exhibited higher and broader tensile stress distribution. Simulating with archwire, the maximal tensile stress of the body of three brackets showed similar results under extreme vertical displacement. However, under extreme horizontal displacement, the body of bracket C exhibited lower maximal tensile stress, while the clip showed higher. And under general horizontal displacement, the body of bracket C presented lowest maximal tensile stress. The clip of bracket A exhibited lower maximal tensile stress rather than the body, while bracket B showed similar maximal tensile stress on the body and the clip.

Tensile stress on the body and the clip results from bracket and archwire interactions is relative and reciprocal, with no definitive answer on which is more clinically critical. When choosing a bracket, factors beyond structural stability such as efficiency of tooth movement, bond strength, aesthetic, patient comfort, and cost could be considered. Therefore, what is more important for clinicians is to recognize this characteristics of structural stability of the brackets under specific conditions and then apply appropriate archwire or mechanics at each stages of the treatment. For developer, using this finite element models to predict structural stability in advance can save significant time and cost compared to relying on conventional intuition-based or trial-and-error process.

Keywords: self-ligating bracket, stress distribution, finite element analysis

Stress distribution according to the design of slot cover in aesthetic passive self-ligating bracket : a finite element analysis

Moonhee Kim

The Graduate School Yonsei University

Department of Dentistry

(Directed by Professor Kee-Joon Lee)

I. INTRODUCTION

More aesthetic orthodontic appliance is ongoing demand from patients. Since their introduction in the 1930s, self-ligating brackets have dominated the clinical orthodontics due to their excellent properties and comfort for both clinicians and patients (Paolo et al., 2022). The clips of conventional self-ligating brackets were made of stainless steel, nickel-titanium or cobalt-chromium alloys, although the body of ceramic self-ligating brackets were aesthetically tooth-colored, the clips were still visible in metallic color (Major et al., 2010; Baxi et al., 2023). There was an attempt to coat the metal clip, however, the white coating material altered the roughness and the friction of metal surface (Albuquerque et al., 2017; Kim et al., 2019). More recently, completely translucent self-ligating brackets are increasingly being used, with the clip portion also made of ceramic material, thus completely clear (Pliska et al., 2014; Shalabh et al., 2023). The precise and exquisite manufacturing of ceramic clips for the delicate opening and closing motions is important and moreover, the potential for fracture due to the nature of the ceramic itself is clinically emphasized for the functionality (Gandini et al., 2013; Carneiro et al., 2015). Fracture of the ceramic bracket contributes to increased chair time and cost, as well as patient discomfort, and the potential health hazard of the aspiration of debris, causing significant inconvenience to both patient and clinician (Ghosh et al., 1995).

To date, no previous investigation has attempted to evaluate the structural stability of aesthetic passive self-ligating brackets with ceramic clip, this study aims to develop a novel method using finite element models. Historically, every time materials advanced from orthodontic bands to full bonded appliances and from metal brackets to ceramic brackets, studies on structural stability supported these advancements (Attia et al., 2018). From this perspective, the primary significance of this study is to address the lack of current research. Thus, the purpose of this study is to compare and evaluate the stress distribution according to the design of slot cover in aesthetic passive self-ligating bracket with ceramic clip using finite element analysis. Herein, 'there is no difference in stress distribution according to the design of slot cover' is established as a null hypothesis.

II. MATERIALS AND METHODS

1. Bracket selection

Each aesthetic passive self-ligating bracket has a slightly different design of slot cover related to the method of coupling the body and the clip of the bracket with specific slider structure (Paolo et al., 2013). Manufacturer provides different terms such as door, slide and clip to describe the slot cover to highlight the characteristics of their products. However, to avoid any confusion in terminology, this study standardize all terms to ‘clip’ which is the most commonly used term in PubMed searches and review articles currently (Baxi et al., 2023).

In this study, three types of maxillary right central incisor passive self-ligating bracket models with 0.022 inch (0.599 mm) slot are investigated: two existing representative brackets with different design of slot cover, keyhole type and drawer type, and a newly designed dovetail type. For keyhole type (bracket A), Clarity Ultra (3M, St. Paul, MN, USA) was reverse-engineered as finite element model and for drawer type (bracket B), Damon Clear2 (Ormco Corporation, Brea, CA, USA) was selected and reverse-modeled. And a newly designed dovetail type (bracket C) which has sufficient width for clinical advantages such as rotation control, while also being structurally resistant to fracture and cost-effective with simplified design was also prepared for finite element analysis. Figure 1 illustrates schematic designs of slot cover of three finite element models.

Figure 1. Schematic designs for three types of maxillary right central incisor passive self-ligating brackets with 0.022 inch slot (A) keyhole type (bracket A), (B) drawer type (bracket B) and (C) dovetail type (bracket C)

2. Finite element model creation

Including these features of slot cover, the shape of the bracket consists of freeform surfaces, so to implement this, a finite element model is created using tetrahedral solid elements using SOLIDWORKS® software (3DEXPERIENCE, Seoul, Republic of Korea, 2022) (Kim et al., 2016; Iriarte et al., 2018; Bernisha et al., 2024). Regions where actual load acting and thus significant deformation and stress occur, such as slot and slider of the body and the clip and its adjacent areas are subjected to a relatively dense element division using finite elements with a length of 0.075 mm. Conversely, the base part at the posterior surface of the body, where deformation and stress are not significant and structural properties such as fracture are not crucial, is subjected to a relatively coarse element division with a length of 0.110 mm to reduce the total number of finite elements and ultimately reduce the entire analytic time. Parts such as intermediate connecting areas are implemented by finite elements with a length of 0.090 mm that allows gradual change in size. Figure 2 presents the final finite element models for this investigation.

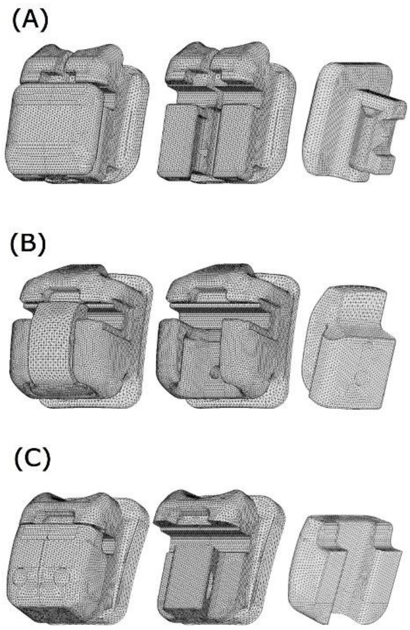

Figure 2. Finite element models for this investigation (A) keyhole type (bracket A), (B) drawer type (bracket B) and (C) dovetail type (bracket C)

3. Tensile stress distribution on the area of interest under specific compressive load

The base material of the bracket, polycrystalline alumina (PCA), is fabricated by mixing metal powders and following sintering process, and its tensile strength is 300 MPa which is about 1/10 of its compressive strength of 3000 MPa (Cai, 2019). In addition, significant compressive load acting on the bracket in clinical situation is rarely pronounced, considering the structural characteristics of the brackets, rather bending or torsion of the body and the clip of the bracket are the primary deformation. Therefore, this investigation only considers the tensile stress generated in the bracket.

In actual clinical situation, it is not straightforward to accurately predict the location and magnitude of the loads acting on the bracket. However, under typical conditions, the expected areas of stress concentration can be approximated as the upper and inner surfaces of the slot, and the inner surface of the slider of the body and the clip. And in the same manner, basically, the bracket is constrained to the posterior surface of the body. Therefore, by applying specific loads and appropriate constraints to these surfaces, the tensile stresses occurring in these parts of the body and the clip can be mutually compared.

4. Clinical simulation

To more practically interpret this structural stability, this investigation also simulates several clinical conditions with orthodontic archwires, divided into extreme and relatively general situations. When archwire is engaged into the bracket in a mal-aligned dentition, it induces displacement and then exerts certain load to the bracket, causing stress. If the stiffness is high or the cross-section is thick, this load on the bracket will increase under the same displacement. In addition, if adjacent teeth are close to each other, meaning the span of the archwire is shorter, the load on the bracket will also increase. Therefore, as shown in Figure 3, after the span of the archwire is fixed at 8 mm which typically determined as an average interbracket distance of the maxillary central incisors in previous studies, the tensile stresses generated by specific vertical and horizontal displacements are surveyed (Schudy and Schudy 1989; Naziris et al., 2019).

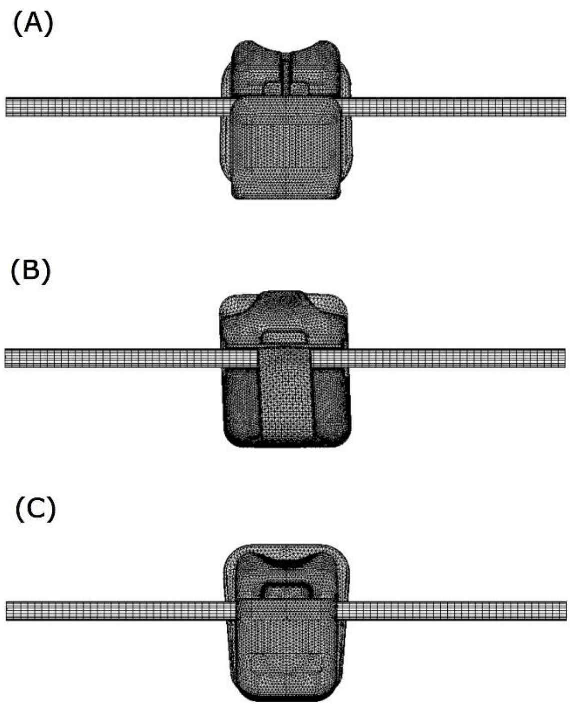

Figure 3. Finite element models with fixed 8 mm length of archwire for clinical simulation (A) keyhole type (bracket A), (B) drawer type (bracket B) and (C) dovetail type (bracket C)

For an extreme clinical simulation using 0.021 × 0.025 - inch stainless steel wire, 8 mm away from the center of the bracket, vertical displacement of 2 and 3 mm is applied respectively for the maximal tensile stress on the body of the bracket. And then, horizontal displacement of 1 and 2 mm is applied to evaluate the maximal tensile stress on both the body and the clip of the bracket. Furthermore, for a relatively typical clinical simulation using 0.016×0.022 – inch stainless steel wire, same with 8 mm away from the center of the bracket, horizontal displacement of 0.5, 1, 1.5 and 2 mm is followed on both the body and the clip of the bracket.

Statistical analysis is not considered for this investigation since it does not involve errors occurring during repeated trials or by intra- and inter-examiner assessments.

III. RESULTS

1. Comparison of tensile stress distribution under specific compressive load

The overall results of tensile stress induced by specific compressive loads are presented in Table 1. Following Figure 4 shows the pattern of this tensile stress distribution induced by specific compressive load of 10 N on the upper surface of the slot of the body. The tensile stress on the upper surface of the slot of bracket C is greater than that of bracket A and B, which implies relatively small curvature angle of the edge. Whereas, Figure 5 demonstrates bracket C exhibits lower and narrower tensile stress distribution than the other two when the inner surface of the slider is loaded .

Table 1. Comparison of tensile stress induced by specific compressive loads

<table>
<tr><th rowspan="2">Part</th><th rowspan="2">Constraint surface</th><th rowspan="2">Load application surface</th><th rowspan="2">Load (N)</th><th colspan="3">Tensile stress (MPa)</th></tr>
<tr><th>Bracket A</th><th>Bracket B</th><th>Bracket C</th></tr>
<tr><td rowspan="2">Body</td><td rowspan="2">Posterior</td><td>Slot upper</td><td rowspan="2">10</td><td>34.2</td><td>27.3</td><td>40.9</td></tr>
<tr><td>Slider inner</td><td>66.3</td><td>35.1</td><td>9.7</td></tr>
<tr><td rowspan="3">Clip</td><td rowspan="2">Slider inner</td><td>Slot inner</td><td rowspan="3">1</td><td>38.5</td><td>24.9</td><td>17.6</td></tr>
<tr><td>Front</td><td>13.4</td><td>12.0</td><td>7.6</td></tr>
<tr><td>Front</td><td>Slider inner</td><td>1.7</td><td>2.1</td><td>4.4</td></tr>
</table>

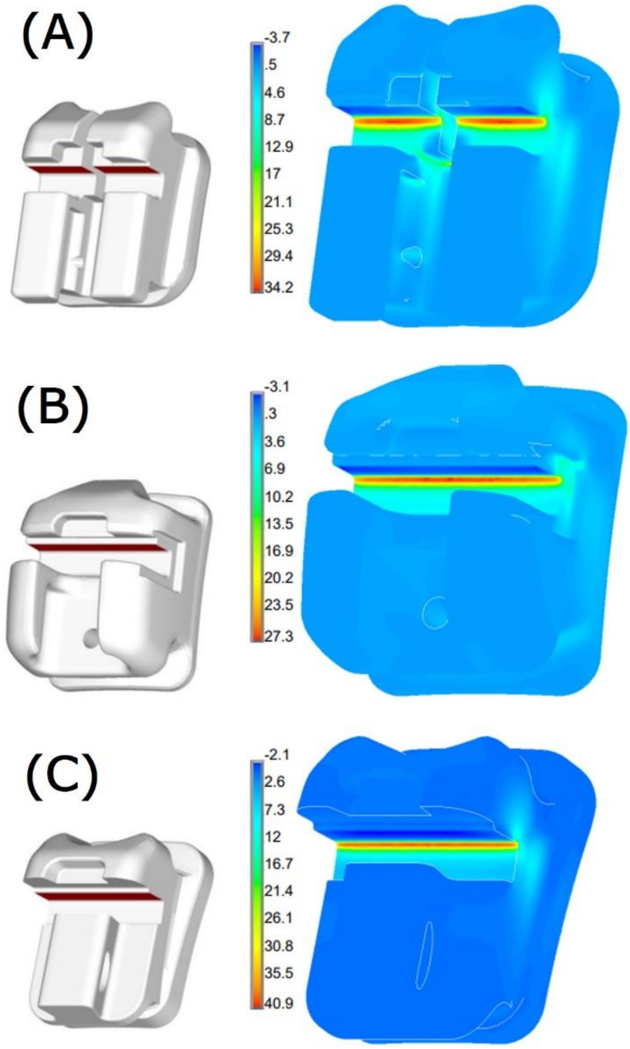

Figure 4. Tensile stress distribution on the body of the bracket induced by a specific compressive load of 10 MPa, load application surface: slot upper (red), constraint surface: posterior (A) keyhole type, (B) drawer type and (C) dovetail type

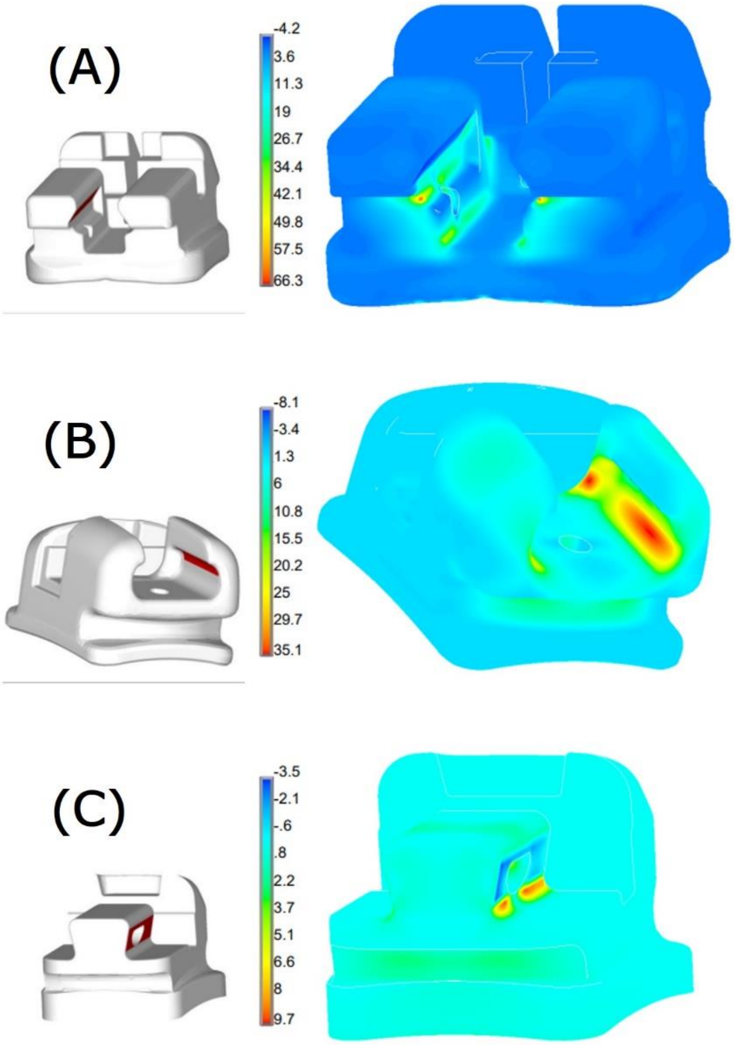

Figure 5. Tensile stress distribution on the body of the bracket induced by a specific compressive load of 10 MPa, load application surface: slider inner (red), constraint surface: posterior (A) keyhole type, (B) drawer type and (C) dovetail type

For the clip, Figure 6 and 7 present that backet C appears the lowest maximal tensile stress on both the inner surface of the slot and the front surface of clip by compressive load of 1 N, when the inner surface of the slider of the clip is constrained.

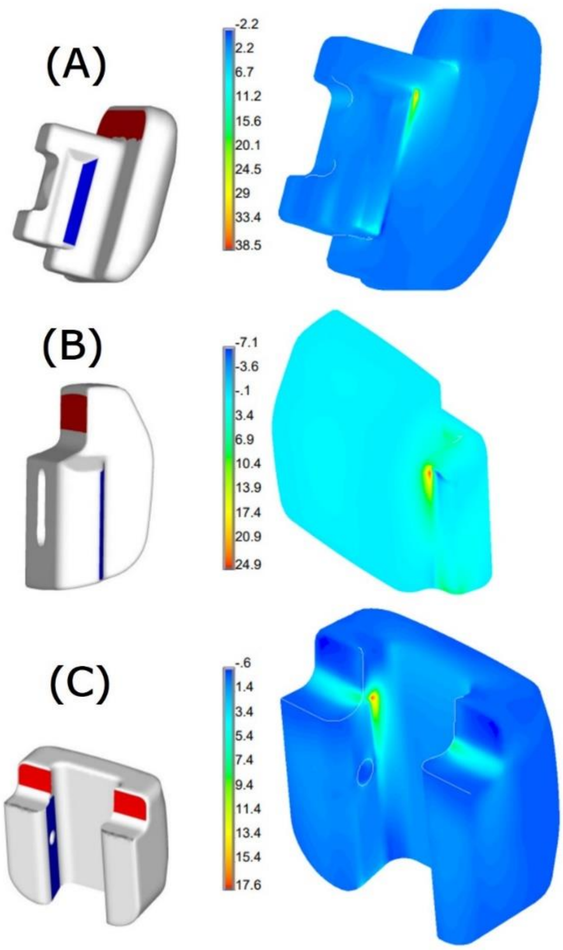

Figure 6. Tensile stress distribution on the clip of the bracket induced by a specific compressive load of 1 MPa, load application surface: slot inner (red), constraint surface: slider inner (A) keyhole type, (B) drawer type and (C) dovetail type

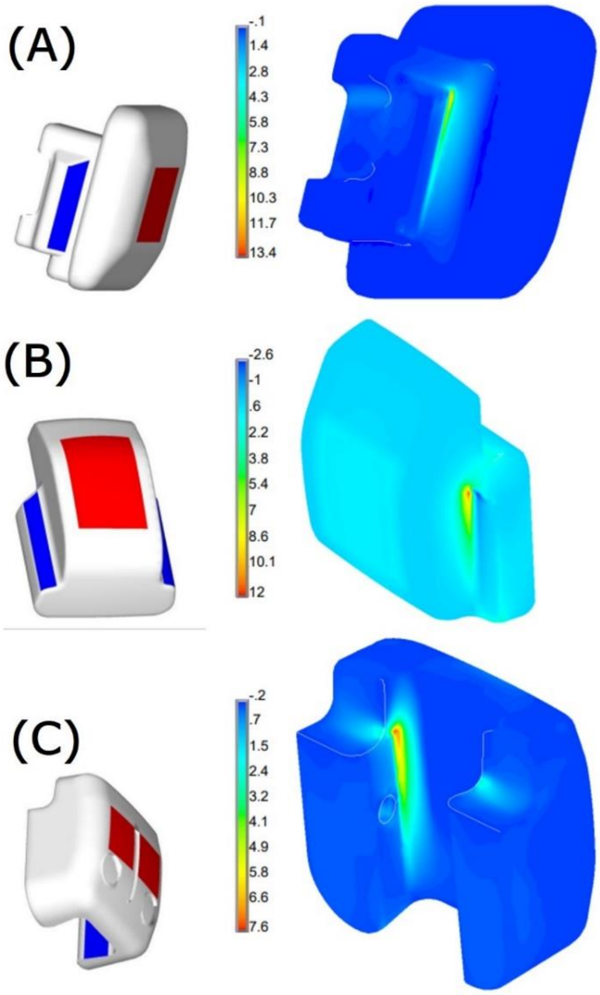

Figure 7. Tensile stress distribution on the clip of the bracket induced by a specific compressive load of 1 MPa, load application surface: front (red), constraint surface : slider inner (A) keyhole type, (B) drawer type and (C) dovetail type

However, Figure 8 shows when load is applied to the inner surface of the slider of the clip, the tensile stress of bracket C is greater than bracket A and B.

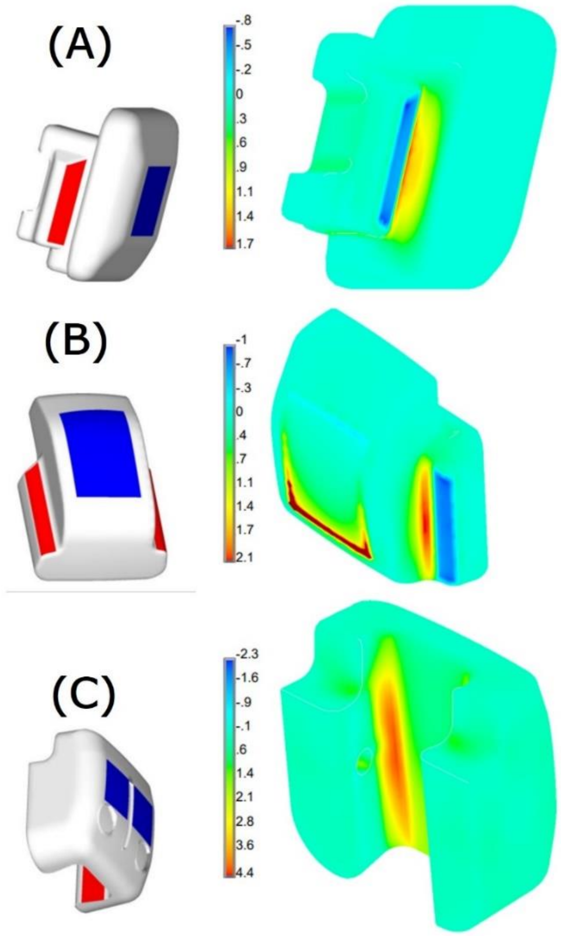

Figure 8. Tensile stress distribution on the clip of the bracket induced by a specific compressive load of 1 MPa, load application surface: slider inner (red), constraint surface: front (A) keyhole type, (B) drawer type and (C) dovetail type

2. Detachment of the body and the clip

The tensile stresses induced by the deformation that would allow mutual detachment of the body and the clip present in Figure 9. For this evaluation, the tensile stresses on the body of the bracket A and B are considered, while the clip of the bracket C is considered according to the design aspect. All the stresses generated by this deformation significantly exceed the stress limit of the material itself, 300 MPa, indicating that the bracket would be fractured before the detachment could occur. Therefore, the possibility of such detachment can be excluded in situations when the bracket structure is maintained.

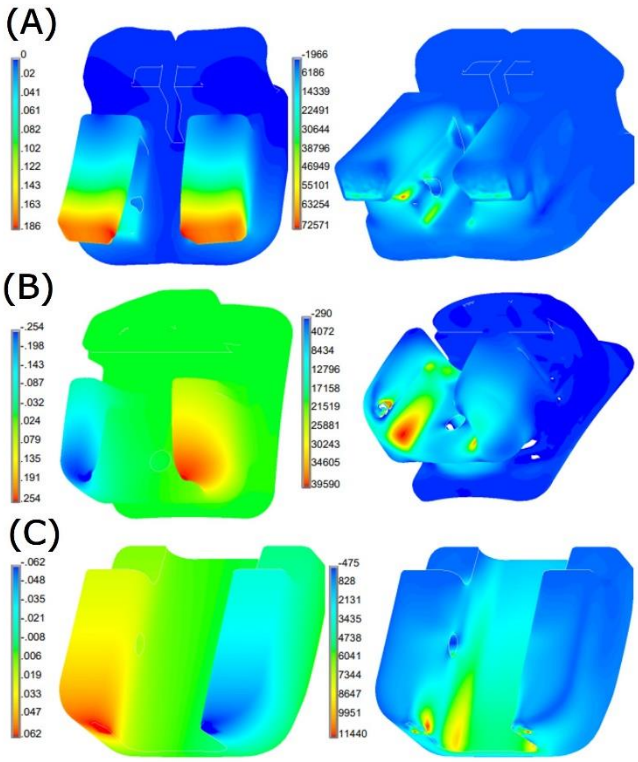

Figure 9. Tensile stress distribution induced by the deformation causing the bottom of the slider to open up (A) keyhole type, (B) drawer type and (C) dovetail type

3. Clinical simulation

3.1. Extreme vertical displacement, on the body

A comparison of the maximal tensile stress on the body of the brackets under extreme vertical displacements is shown in Table 2. The body of three brackets shows similar tensile stress distribution under extreme vertical displacement by full-sized stiff wire. Only by 2 mm vertical displacement of 0.021 × 0.025 - inch stainless steel wire, the maximal tensile stress on the body of the brackets already reaches 80% of the allowable tensile strength of 300 MPa, and this displacement may lead to failure of the bracket itself to maintain structural stability. Therefore, in extreme situations, there is no difference between the brackets. On the other hand, it can be noted that the maximal tensile stress on the body of the bracket does not increase proportionally to the amount of vertical displacement of archwire, rather increases more significantly than the displacement ratio.

Table 2. Maximal tensile stress on the body of the brackets by extreme vertical displacement using 0.021 × 0.025 - inch stainless steel wire

Vertical displacement (mm)	Maximal tensile stress (MPa)		
	Bracket A	Bracket B	Bracket C
2	260	241	264
3	414	407	416

Figures 10 and 11 depict the tensile stress distribution on the body of the bracket by extreme vertical displacement of 2 and 3 mm using 0.021 × 0.025 - inch stainless steel wire. All of the following graphics of stress distribution are visualized with and without outlines of finite elements. In the figure without outlines, the distribution of the maximal stress can be observed relatively clearly, while the representation of the shape of the brackets is ambiguous. Conversely, in the figure with outlines, the opposite. Therefore, by comparing two forms, the pattern and the location of the stress distributions can be identified distinctly.

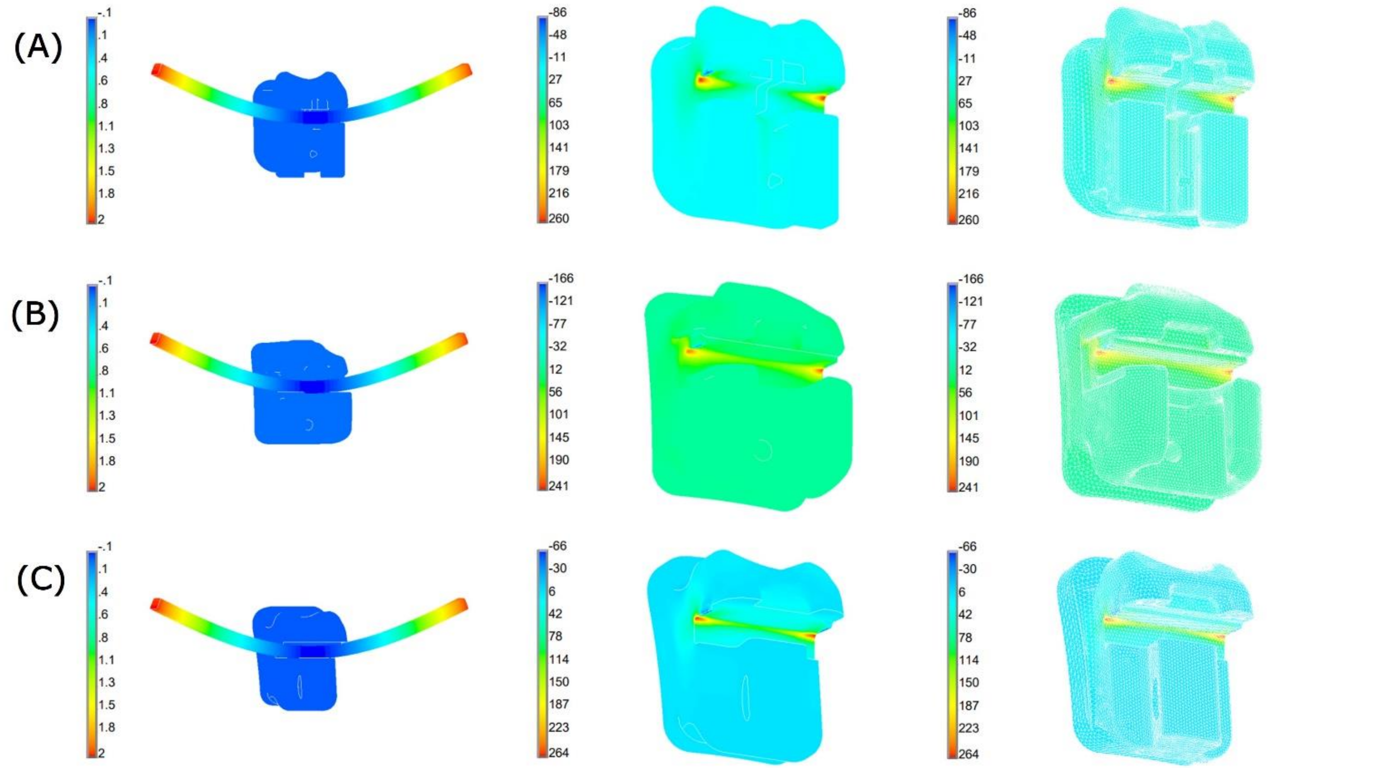

Figure 10. Graphical display of the tensile stress distribution on the body of the brackets by extreme vertical displacement of 2 mm using 0.021 × 0.025 - inch stainless steel wire with and without outlines of finite element (A) keyhole type, (B) drawer type and (C) dovetail type

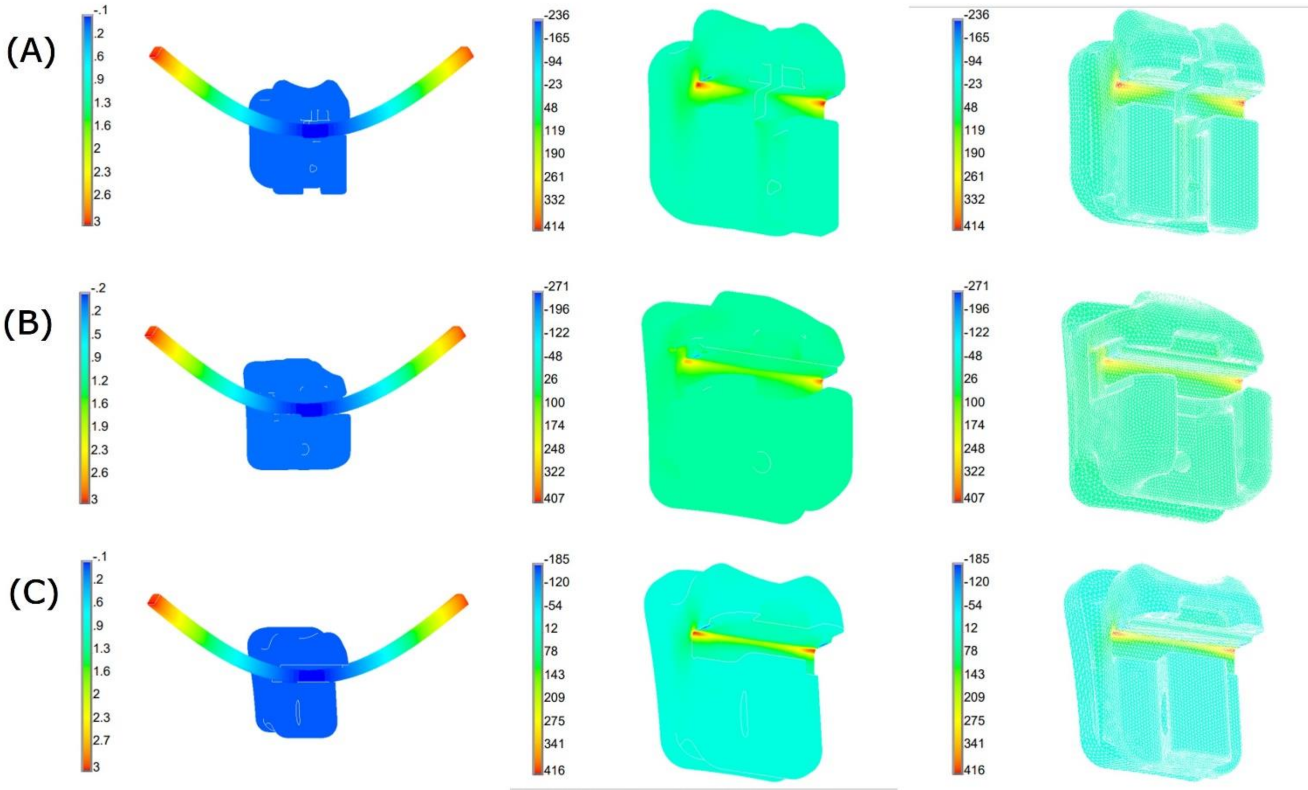

Figure 11. Graphical display of the tensile stress distribution on the body of the brackets by extreme vertical displacement of 3 mm using 0.021 × 0.025 - inch stainless steel wire with and without outlines of finite element (A) keyhole type, (B) drawer type and (C) dovetail type

3.2. Extreme horizontal displacement, on the body and the clip

The maximal tensile stresses on the body and the clip of the brackets under extreme horizontal displacements by same 0.021 × 0.025 - inch stainless steel wire are summarized in Table 3. The maximal tensile stress on the body of bracket C is lower than that of the other brackets when the same amount of horizontal displacement is applied. Moreover, the value of bracket C by horizontal displacement of 2 mm is lower than that of bracket A by horizontal displacement of 1 mm. Only by horizontal displacement of 1 mm using 0.021 × 0.025 - inch stainless steel wire, the maximal tensile stress on the body of bracket A and B already exceeds 80%, especially bracket A almost reaches the allowable tensile strength of 300 MPa. In such an extreme situation, the body of bracket C has better structural stability regarding fracture. However, the maximal tensile stress on the clip of bracket C is higher than other two. And the maximal tensile stress of the clip of bracket A and B is lower than that of the body under the same extreme horizontal displacement, whereas the body of bracket C is lower than that of the clip. Meanwhile under such extreme conditions, horizontal displacement over 2 mm using 0.021 × 0.025 - inch stainless steel wire, all the clips of the brackets could be fractured. And compared with the same amount of 2 mm displacement, the maximal tensile stresses on the body of all brackets is higher when horizontal displacement is applied than vertical displacement.

Table 3. Maximal tensile stress on the body and the clip of the brackets by extreme horizontal displacement using 0.021 × 0.025 - inch stainless steel wire

Part	Horizontal displacement (mm)	Maximal tensile stress (MPa)		
		Bracket A	Bracket B	Bracket C
Body	1	297	246	127
	2	668	549	287
Clip	1	233	222	427
	2	473	451	1018

Following Figure 12 and 13 present the corresponding displays for the tensile stress distribution on the body and the clip of the brackets by extreme horizontal displacement of 1 and 2 mm using 0.021 × 0.025 - inch stainless steel wire. Regarding the outlines, same as in the previous explanation.

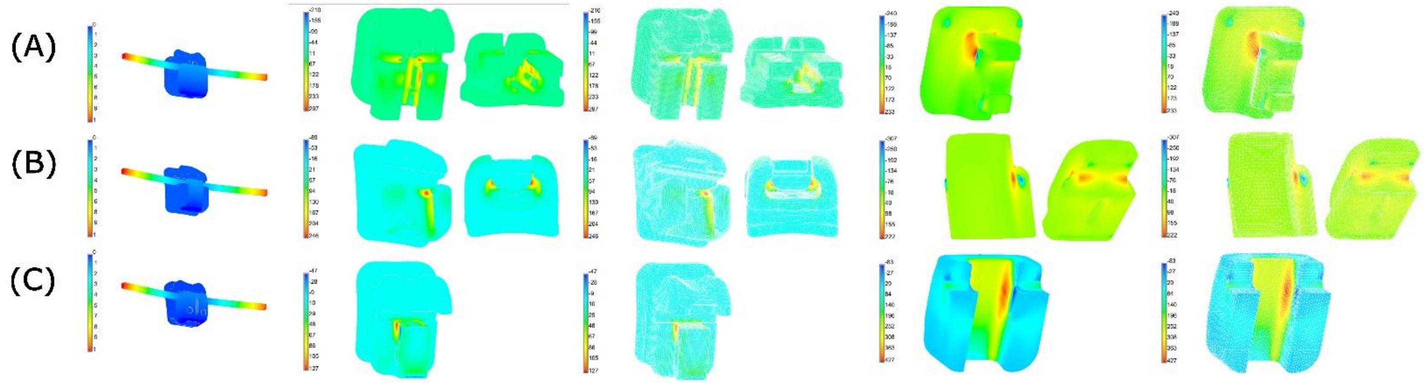

Figure 12. Graphical display of the tensile stress distribution on the body and the clip of the brackets by extreme horizontal displacement of 1 mm using 0.021 × 0.025 - inch stainless steel wire with and without outlines of finite element (A) keyhole type, (B) drawer type and (C) dovetail type

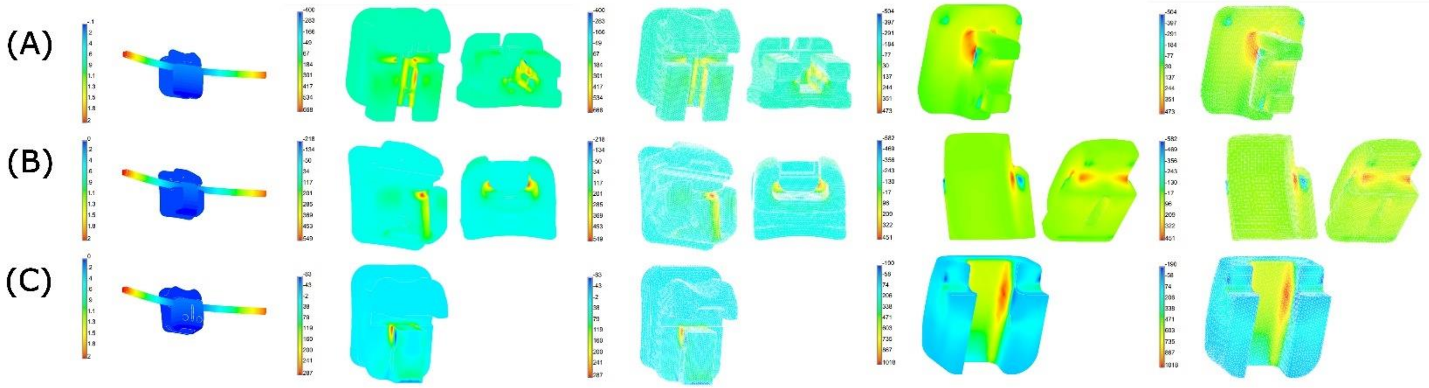

Figure 13. Graphical display of the tensile stress distribution on the body and the clip of the brackets by extreme horizontal displacement of 2 mm using 0.021 × 0.025 - inch stainless steel wire with and without outlines of finite element (A) keyhole type, (B) drawer type and (C) dovetail type

3.3. General horizontal displacement, on the body and the clip

Table 4 and Figure 14 indicate the tensile stresses on the body and the clip of the brackets by horizontal displacement under clinically relevant condition using 0.016 × 0.022 - inch stainless steel wire at a more subdivided scale. For every amounts of horizontal displacement, the stress on the body of bracket C is the lowest, especially less than half that of bracket A. For horizontal displacement exceeding 2 mm, the bodies of bracket A and B are prone to be fractured, whereas the stress on the body of bracket C is still below the allowable tensile stress. However, stress on the clip of bracket C is higher than the others, while the clips of bracket A and B are likely to maintain their structural stability even with horizontal displacements greater than 1.5 mm. In particular, bracket A exhibits lower stress on the clip than the body for all horizontal displacements.

Table 4. Maximal tensile stress on the body and the clip of the brackets by general horizontal displacement using 0.016 × 0.022 - inch stainless steel wire

Part	Horizontal displacement (mm)	Maximal tensile stress (MPa)		
		Bracket A	Bracket B	Bracket C
Body	0.5	75	68	34
	1	162	130	69
	1.5	256	208	109
	2	360	292	156
Clip	0.5	71	70	107
	1	137	131	221
	1.5	203	193	359
	2	277	261	519

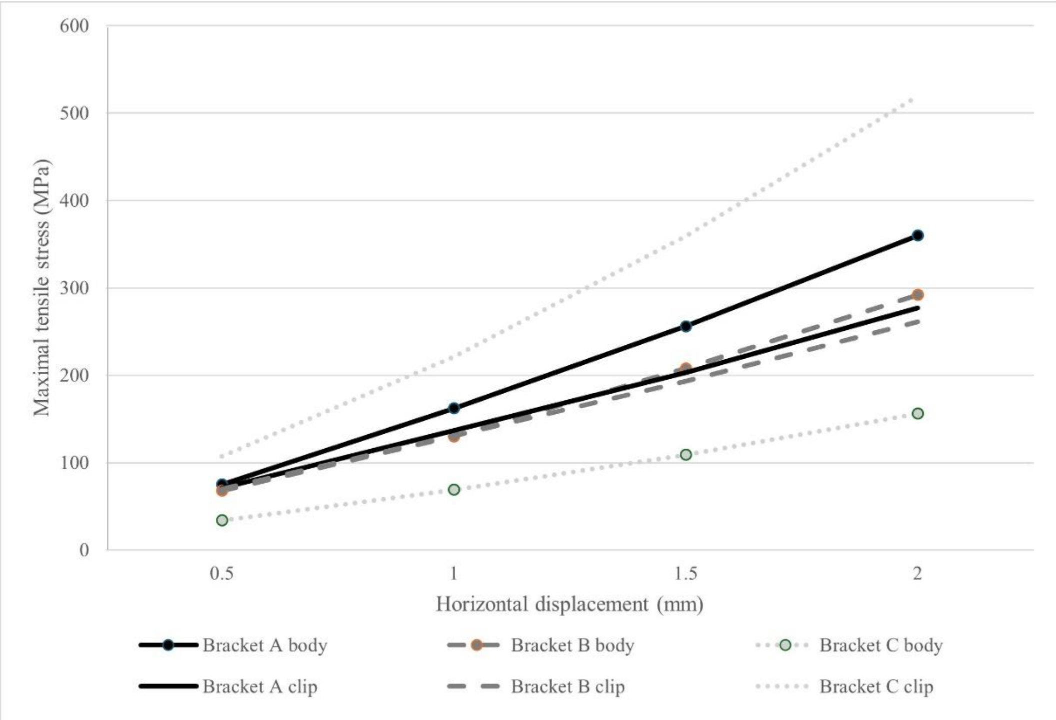

Figure 14. Comparison of the maximal tensile stress on the body and the clip of the brackets by general horizontal displacement using 0.016 × 0.022 - inch stainless steel wire

Figure 15,16,17 and 18 present the corresponding displays of the tensile stress distribution on the body and the clip of the brackets by general horizontal displacement of 0.5,1,1.5 and 2 mm using 0.016 × 0.022 - inch stainless steel wire. Regarding the outlines, also same as in the previous explanation.

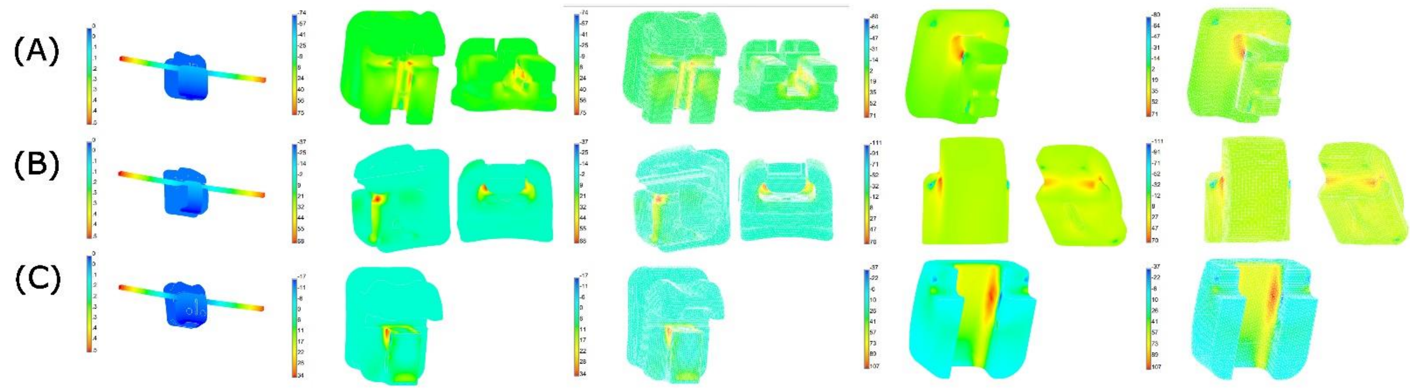

Figure 15. Graphical display of the tensile stress distribution on the body and the clip of the brackets by general horizontal displacement of 0.5 mm using 0.016 × 0.022 - inch stainless steel wire with and without outlines of finite element (A) keyhole type, (B) drawer type and (C) dovetail type

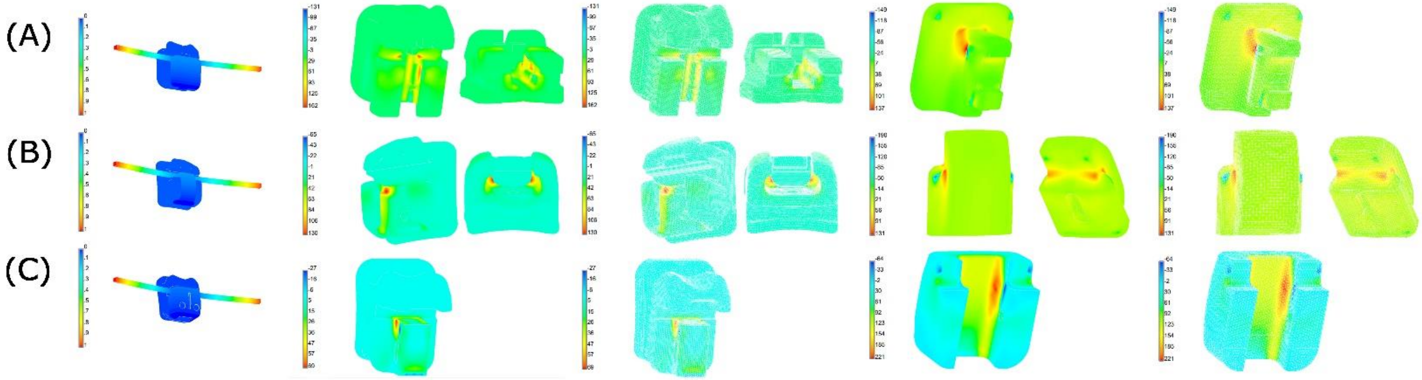

Figure 16. Graphical display of the tensile stress distribution on the body and the clip of the brackets by general horizontal displacement of 1 mm using 0.016 × 0.022 - inch stainless steel wire with and without outlines of finite element (A) keyhole type, (B) drawer type and (C) dovetail type

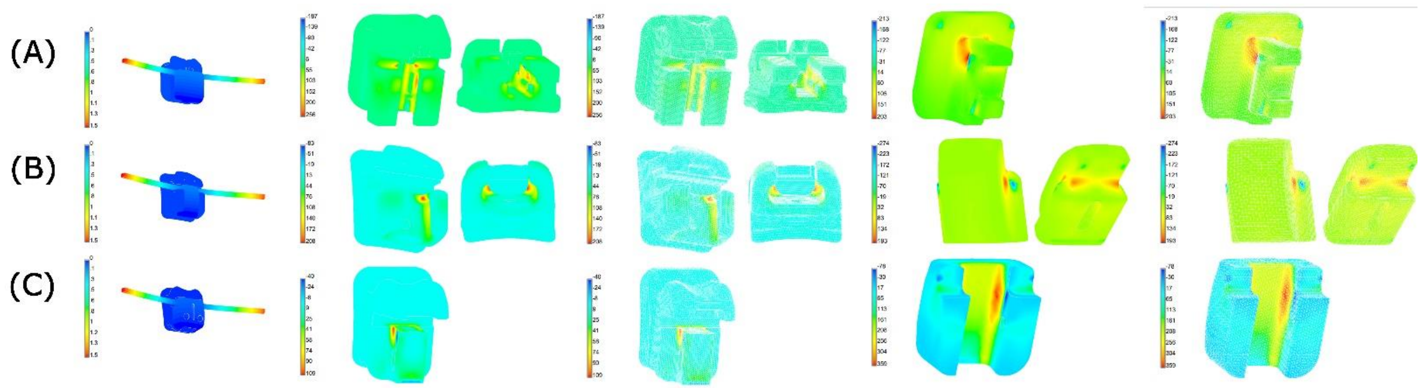

Figure 17. Graphical display of the tensile stress distribution on the body and the clip of the brackets by general horizontal displacement of 1.5 mm using 0.016 × 0.022 - inch stainless steel wire with and without outlines of finite element (A) keyhole type, (B) drawer type and (C) dovetail type

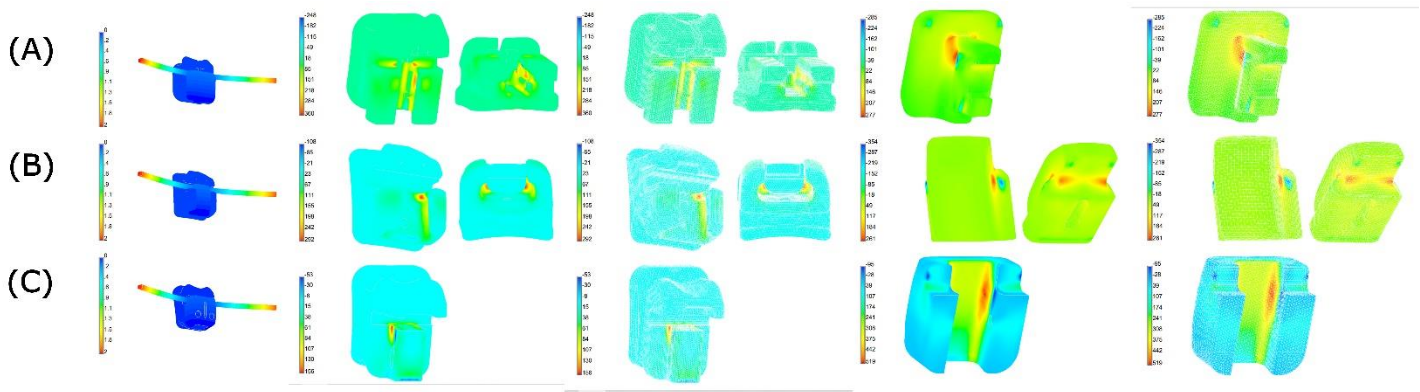

Figure 18. Graphical display of the tensile stress distribution on the body and the clip of the brackets by general horizontal displacement of 2 mm using 0.016 × 0.022 - inch stainless steel wire with and without outlines of finite element (A) keyhole type, (B) drawer type and (C) dovetail type

IV. DISCUSSION

It is difficult to specify a particular load for evaluating the structural stability of bracket (Melenka et al., 2013). And this study alone cannot comprehensively assess the overall structural stability. However, the comparison of the tensile stress distribution under identical specific compressive loads revealed that, the body of bracket C, especially the slider, showed lower tensile stress, while relatively higher tensile stress with wider distribution area was observed in the clip. Thus, null hypothesis was rejected due to differences in this stress distribution in aesthetic passive self-ligating bracket according to the design of slot cover.

Subsequent experiments to demonstrate the potential for the detachment of the body and the clip under the deformation causing the bottom of the slider to spread apart, indicate all of the brackets would undergo fracture before the detachment occurs, this is not relevant in clinical situation (Thomas et al., 2013).

The comparison of the maximal tensile stress on the body of the brackets under extreme vertical displacements using 0.021 × 0.025 - inch stainless steel wire showed similar results between the brackets. Since the tensile stress did not increase linearly with the amount of displacement, clinicians should have a caution in such severe conditions.

On the other hand, under extreme horizontal displacements, three brackets presented different tensile stress distribution according to the design. By each extreme horizontal displacement, the maximal tensile stress on the body of bracket C was the lowest. Under extreme conditions of horizontal displacement exceeds 1mm, the bodies of bracket A and B were at high risk of losing structural stability. Especially the maximal tensile stress of the body of bracket A almost reached the allowable limit of 300 MPa only by horizontal displacement of 1 mm using 0.021 × 0.025 - inch stainless steel wire, and even greater than that of bracket C under horizontal displacement of 2mm.

The maximal tensile stress on the body of the brackets was higher under the same amount of horizontal displacement than under vertical displacement, which implies that the structural stability of the body under horizontal displacement is relatively more vulnerable in a simple comparison when applying edgewise mechanics. Fracture of the ceramic bracket is detrimental for both clinicians and patients, clinicians strive to eliminate such a heavy displacement (Joydeep et al., 1995).

For the clips, when subjected to extreme horizontal displacement of 2 mm, the maximal tensile stress on the clip of all three brackets exceeded the allowable tensile stress, making them highly susceptible to fracture. Comparing extreme horizontal displacement of 1 mm using 0.021 × 0.025 - inch stainless steel wire, the maximal tensile stress on the clip of bracket C with a newly designed dovetail type was relatively high.

In more general and similar to actual clinical conditions using 0.016 × 0.022 - inch stainless steel wire, only horizontal displacement was investigated at a more subdivided scale. The body of bracket C showed the lowest maximal tensile stress for every displacements, especially less than half of the body of bracket A. Contrary to bracket A and B, only the body of bracket C may maintain structural stability under horizontal displacement of 2 mm. However, the clip of bracket C was likely to be fractured under horizontal displacement over 1.5 mm, while the clip of bracket A and B still below their allowable limits, even if there is a possibility that the bodies of bracket A and B have already been fractured. Particularly, the clip of bracket A with a keyhole design presented lower stress rather than the body for all horizontal displacements.

Based on the overall comparison of the tensile stresses of three brackets from a structural engineering perspective regarding fracture, bracket A and B showed relative stabilities on the clip, while bracket C exhibited superiority on the body, especially on the slider. However, it is not entirely sufficient to evaluate the overall stability and performance of the brackets solely by comparing this tensile stress distribution under specific loads. Additionally, there is no definitive answer as to which is more critical compartment in clinical situation, the body or the clip. For instance, if a clip of the bracket is fractured in an extreme or accidental situation, clinician may immediately remove the fractured clip and tie the wings with the ligature wire to continue orthodontic force (Sha et al., 2018). In this case, it rather may help to overcome a pointed out limitation of passive self-ligating bracket, especially in areas that require torque expression such as maxillary incisors (Liu et al., 2013; Bernisha et al., 2024; Saraiva et al., 2024). Contrary, if a body of the bracket is fractured, clinician may remove the remnants of the body of the bracket and remained adhesive resin, then simply re-bond a new bracket (Flores et al., 1990; Stocker et al., 2022). In this case, clinician should select an appropriate archwire with superelasticity or apply a single force first, considering the structure stability of the bracket refer to this investigation or their own empirical basis (Major et al., 2011; Moradinejad et al., 2021).

When choosing a bracket, structural stability is not the only criterion, in fact there are many other factors to consider, including efficiency of tooth movement, bond strength, aesthetics, patient comfort, and cost (Sfondrini et al., 2011; Melenka et al., 2013; Vartolomei et al., 2022). Therefore, what is more important for clinicians is to recognize this characteristics of structural stability of the brackets under specific conditions and apply proper archwire or mechanics at every stages of the orthodontic treatment (Lopes et al., 2023). And for developers, using this finite element models to predict the structural stability in advance when preparing new or modified designs that involve replacing existing slider structures or coupling methods of the body and the clip, can save significant time and cost compared to relying on conventional intuition-based or trial-and-error process.

V. CONCLUSION

In comparison of visualized and numerically calculated stress distribution of the body and the clip of three aesthetic passive self-ligating brackets under specific load condition, using reverse engineered finite element models, the body of bracket C with a dovetail design showed relatively low tensile stress.

In clinically extreme simulations, bracket A, B and C exhibited similar maximal tensile stress under vertical displacement, while the body of bracket C, the clip of bracket A with a keyhole design and the clip of bracket B with a drawer design presented relatively low maximal tensile stress under horizontal displacement. And in more general and clinically relevant simulations, the body of bracket C and the clip of bracket A showed relatively low maximal tensile stress under horizontal displacement.

Thus in the case of the newly designed bracket C, some modifications to supplement the stability of the clip structure regarding fracture should be considered.

VI. REFERENCES

Attia KH, Elkordy SA, ElKoussy M, Abouelezz AM (2018). Are self-ligating brackets' slots dimensions accurate? *J Ortho 16(4): 613-622.*

Baxi S, Tripathi AA, Bhatia V, Prasad Dubey M, Kumar P, Bagde H (2023). Self-ligating bracket systems: a comprehensive review. *Cureus. 15(9):e44834.*

Bernisha RP, Mishra G, Pradeep Raj G, Chitra P (2024). Incisor torque expression characteristics in two passive self-ligating brackets placed at different heights. A finite element investigation. *J Oral Biol Craniofac Res. 14(1): 98-106.*

Cai Y (2019). A three-dimensional finite element analysis of the effect of archwire characteristics on the self-ligating orthodontic tooth movement of the canine. *Technol Health Care. 27(S1): 195-204.*

Flores DA, Caruso JM, Scott GE, Jeiroudi MT (1990). The fracture strength of ceramic brackets: a comparative study. *Angle Orthod. 60(4): 269-276.*

Gandini P, Orsi L, Sfondrini MF, Scribante A (2013). Opening and closure forces of sliding mechanisms of different self-ligating brackets. *J Appl Oral Sci. 21(3): 231-234.*

Ghosh J, Nanda RS, Duncanson MG, Currier GF (1995). Ceramic bracket design: An analysis using the finite element method. *Am J Orthod Dentofac Orthop. 108(6): 575-582.*

Iriarte AJ, Ortiz S, Cubides-Flechas K, Olaya C, Jaimes-Monroy G (2018). Sliding resistance of rectangular vs. beveled archwires in two self-ligating brackets: a finite element study. *Acta Odontol Latinoam. 31(3): 149-155.*

Kim KS, Han SJ, Lee TH, Park TJ, Choi S, Kang YG, Park KH (2019). Surface analysis of metal clips of ceramic self-ligating brackets. *Korean J Orthod. 49(1): 12-20.*

Kim SJ, Kwon YH, Hwang CJ (2016). Biomechanical characteristics of self-ligating brackets in a vertically displaced canine model: a finite element analysis. *Orthod Craniofac Res. 19(2): 102-113.*

Liu X, Ding P, Lin J (2013). Effects of bracket design on critical contact angle. *Angle Orthod. 83(5): 877-884.*

Lopes GC, Watinaga GK, Guimarães AS, Rocha Valadas LA, Ramacciato J (2023). Self-ligating brackets do not reduce discomfort or pain when compared to conventional orthodontic appliances in Class I patients: a clinical study. *Angle Orthod. 93(4): 398-402.*

Major TW, Carey JP, Nobes DS, Major PW (2010). Orthodontic bracket manufacturing tolerances and dimensional differences between select self-ligating brackets. *J Dent Biomech. 27: 781321.*

Major TW, Carey JP, Nobes DS, Heo G, Major PW (2011). Measurement of plastic and elastic deformation due to third-order torque in self-ligated orthodontic brackets. *Am J Orthod Dentofac Orthop. 140(3): 326-339.*

Major TW, Carey JP, Nobes DS, Heo G, Major PW (2012). Deformation and warping of the bracket slot in select self-ligating orthodontic brackets due to an applied third order torque. *J Orthod. 39(1): 25-33.*

Major TW, Carey JP, Nobes DS, Heo G, Melenka GW, Major PW (2013). An investigation into the mechanical characteristics of select self-ligated brackets at a series of clinically relevant maximum torquing angles: loading and unloading curves and bracket deformation. *Eur J Orthod. 35(6): 719-729.*

Melenka GW, Nobes DS, Carey JP, Major PW (2013). Three-dimensional deformation comparison of self-ligating brackets. *Am J Orthod Dentofac Orthop. 143(5): 645-657.*

Melenka GW, Nobes DS, Major PW, Carey JP (2013). Three-dimensional deformation of orthodontic brackets. *J Dent Biomech. 4:1758736013492529.*

Moradinejad M, Ghorani N, Heidarpour M, Noori M, Rakhshan V (2021). Effects of a ceramic active self-ligating bracket on retraction/tipping/rotation of canine, premolar mesialization, and transverse arch dimensions: A preliminary single-blind split-mouth randomized clinical trial. *Dent Res J. 21(18):81*.

Naziris K, Piro NE, Jäger R, Schmidt F, Elkholy F, Lapatki BG (2019). Experimental friction and deflection forces of orthodontic leveling archwires in three-bracket model experiments. *J Orofac Orthop. 80(5): 223–235.*

Pliska BT, Fuchs RW, Beyer JP, Larson BE (2014). Effect of applied moment on resistance to sliding among esthetic self-ligating brackets. *Angle Orthod. 84(1): 134-139.*

Saraiva PC, Cruz MH, Medeiros IS, Bozelli JV, Neto JR, Paiva JB (2024). Comparison of torque expression among passive self-ligating brackets with different slot depths: An in vitro study. *J Ortho. 22(2): 100866.*

Schudy GF, Schudy FF (1989). Intrabracket space and interbracket distance: critical factors in clinical orthodontics. *Am J Orthod Dentofacial Orthop. 96(4): 281-294.*

Sfondrini MF, Gatti S, Scribante A (2011). Shear bond strength of self-ligating brackets. *Eur J*

Orthod. 33(1): 71-74.

Sha HN, Choi SH, Yu HS, Hwang CJ, Cha JY, Kim KM (2018). Debonding force and shear bond strength of an array of CAD/CAM-based customized orthodontic brackets, placed by indirect bonding- An In Vitro study. *PLoS One. 11;13(9).*

Stocker T, Li H, Bamidis EP, Baumert U, Hoffmann L, Wichelhaus A, Sabbagh H (2022). Influence of normal forces on the frictional behavior in tribological systems made of different bracket types and wire dimensions. *Dent Mater J. 41(3): 402-413.*

Vartolomei AC, Ghiga DV, Serbanoiu DC, Moldovan M, Cuc S, Pacurar M, Pollmann MCF (2022). Comparative evaluation of two bracket systems' bond strength: conventional and self-ligating. *Dent J. 21(10):196.*

국문요약

심미적 자가 결찰 브라켓의 덮개 형태에 따른 응력 분포

: 유한 요소 분석

(지도 교수 : 이 기 준)

연세대학교 대학원 치의학과

김 문 희

전체 세라믹으로 제작된 심미적 자가 결찰 브라켓이 널리 사용되면서, 소재 자체의 특성상 파절과 연관된 응력 분포에 대한 평가가 필요하다. 덮개 형태가 다른 대표적인 브라켓 2종, 즉 keyhole type (브라켓 A)과 drawer type (브라켓 B)을 각각 역 모델링한 유한 요소 모델과, 임상적으로 회전 조절 등에 유리할 만큼 충분한 폭경을 가지면서도 구조적으로 파절 저항 및 제작 비용 절감에 유리하도록 수정 설계한 dovetail type (브라켓 C)의 유한 요소 모델, 총 3종의 응력 분포 및 그 특징을 시각화 및 수치화하여 비교 평가하였다.

임의의 압축 하중에 의해 주요 관심 부위에 발생하는 인장 응력을 비교 하였으며, 실제 교정용 호선과의 상호 작용을 통해 발생하는 최대 인장 응력을 극단적인 수직 변위와 수평

변위로 나누어 조사하였고, 일반적인 임상 상황과 유사한 조건의 수평 변위를 보다 세분화하여 조사하였다.

임의의 압축 하중에 의한 인장 응력의 분포를 상호 비교한 결과, 브라켓 C의 본체, 특히 슬라이더 부위의 낮은 인장 응력 분포가 확인 되었고, 상대적으로 클립은 인장 응력이 다소 높고 분포 영역도 넓은 경향을 보였다. 한편, 호선을 이용하여 임상 조건을 구현했을 때, 극단적인 수직 변위에서는 브라켓 3종 본체의 최대 인장 응력에서 큰 차이가 없었으며, 극단적인 수평 변위에서는 브라켓 C 본체의 최대 인장 응력이 낮았고, 반대로 클립의 최대 인장 응력은 높았다. 보다 일반적인 임상 조건의 수평 변위에서는 브라켓 C 본체가 가장 낮은 최대 인장 응력을 보였다. 브라켓 A는 본체보다 클립이 더 낮은 최대 인장 응력을, 브라켓 B는 본체와 클립이 거의 유사한 결과를 보였다.

브라켓과 호선의 상호 작용으로 발생한 본체와 클립의 응력은 상호적일 수 있으며 따라서 어느 부위의 구조적 안정성이 더 중요한지 절대적 우위는 없다. 또한 브라켓 선택 시에는 단순히 구조적 안정성 외에도 치아 이동의 효율성, 접착 강도, 심미성, 편안함 및 비용 등 많은 요소들이 동시에 고려된다. 그러므로 이러한 다양한 조건에서의 파절과 연관된 구조적 안정성을 잘 이해하고, 각 치료 단계에서 이를 고려하여 적절한 호선을 선택하여 교정력을 적용하는 과정이 중요하다고 하겠다. 한편, 본 유한 요소 모델을 통한 연구 방법은 브라켓의 개발 및 수정 과정에서 경험적 근거나 시행착오를 반복하던 기존의 방식 대신, 미리 응력 분포를 확인하고 계산하여 구조적 안정성을 예상하고 보완할 수 있는 구조물 등을 추가 설계하는 데 도움을 줄 수 있을 것이다.

핵심이 되는 말: 자가 결찰 브라켓, 응력 분포, 유한 요소 분석